

# Experimental demonstration of non-bilocality with truly independent sources and strict locality constraints

Qi-Chao Sun<sup>1,2,5</sup>, Yang-Fan Jiang<sup>1,2,5</sup>, Bing Bai<sup>1,2,5</sup>, Weijun Zhang<sup>3</sup>, Hao Li<sup>3</sup>, Xiao Jiang<sup>1,2</sup>, Jun Zhang<sup>1,2</sup>, Lixing You<sup>3</sup>, Xianfeng Chen<sup>4</sup>, Zhen Wang<sup>3</sup>, Qiang Zhang<sup>1,2\*</sup>, Jingyun Fan<sup>1,2\*</sup> and Jian-Wei Pan<sup>1,2\*</sup>

**The ongoing interest in creating a secure global quantum network culminated recently in the demonstration of transcontinental quantum communication<sup>1</sup>. There is a pressing need to examine the properties attached to a quantum network architecture from multiple perspectives, including physics foundations<sup>2</sup>, communication security<sup>3</sup>, the efficient use of resources and innovative technological applications<sup>4,5</sup>. Here, we present an experimental realization of a five-node quantum network, in which quantum sources at two nodes deliver entangled photon pairs to three measurement nodes. With relevant events between five nodes separated space-like, we demonstrate violation of the Bell inequality and bilocal inequality<sup>6</sup>, with the locality, measurement independence and quantum source independence loopholes closed simultaneously in a quantum network. This experimental realization may be valuable for the design and implementation of future quantum networks.**

Quantum non-locality is incompatible with local realism<sup>7,8</sup>. Several recent Bell test experiments disproved (single) local hidden variable models by closing detection, locality and measurement independence loopholes simultaneously in a two-party configuration<sup>9–12</sup>. Discussions of this may be further enriched when applied to a quantum network setting in terms of fundamental science<sup>13–16</sup> and realistic applications, as quantum non-locality is a rich resource for many information processing tasks, such as device-independent quantum information processing applications<sup>4,5</sup>.

Consider the simplest quantum network shown in Fig. 1, where source  $S_1$  distributes Bell state  $|\Phi^+\rangle_{AB} = \frac{1}{\sqrt{2}}(|H\rangle_A|H\rangle_B + |V\rangle_A|V\rangle_B)$  between Alice and Bob and source  $S_2$  distributes Bell state  $|\Phi^+\rangle_{BC} = \frac{1}{\sqrt{2}}(|H\rangle_B|H\rangle_C + |V\rangle_B|V\rangle_C)$  between Bob and Charlie, where  $|H\rangle$  and  $|V\rangle$  denote the horizontal and vertical polarization quantum states, respectively. Entanglement swapping is realized conditioning on the Bell state measurement (BSM) by Bob. The particles held by Alice and Charlie have never interacted before becoming entangled<sup>17</sup>. Note that the recent loophole-free experimental realizations of violating the Bell inequality exclude any hidden variables that may have been created along with the birth of the entangled photons state used in the tests<sup>10,11</sup>. We adopt this assumption in our experiment. As shown in Fig. 1, the two-state creation events at the two sources are independent of one another and the respective quantum state measurement events. Each state creation event is independently

assigned a local hidden variable to carry the exact state information; that is,  $\lambda_1$  is created in source  $S_1$  and passed to Alice and Bob, and  $\lambda_2$  is created in source  $S_2$  and passed to Bob and Charlie. According to local hidden variable theories, the measurement outcomes  $a$ ,  $b$  and  $c$  of Alice, Bob and Charlie at the three nodes are (statistically) predetermined for measurement setting choices  $x$ ,  $y$ ,  $z$  and local hidden variables  $\lambda_1$  and  $\lambda_2$ , respectively, such that  $a = a(x, \lambda_1)$ ,  $b = b(y, \lambda_1, \lambda_2)$  and  $c = c(z, \lambda_2)$ . The tripartite probability distribution under the bilocal hidden variable assumption can be given by

$$P(a, b, c|x, y, z) = \int d\lambda_1 d\lambda_2 \rho(\lambda_1, \lambda_2) P(a|x, \lambda_1) P(b|y, \lambda_1, \lambda_2) P(c|z, \lambda_2) \quad (1)$$

where  $P(a|x, \lambda_1)$ ,  $P(b|y, \lambda_1, \lambda_2)$  and  $P(c|z, \lambda_2)$  are the probabilities of local measurements at the three nodes, respectively. The independent sources and locality condition require the probability distribution of local hidden variables to be factorable,  $\rho(\lambda_1, \lambda_2) = \rho(\lambda_1)\rho(\lambda_2)$  with  $\int d\lambda_1 \rho(\lambda_1) = 1$  and  $\int d\lambda_2 \rho(\lambda_2) = 1$ . Others have shown that the bilocal hidden variable model sets a constraint to the joint measurement<sup>6,8</sup>, which appears in the form of

$$\mathcal{B} = \sqrt{|I|} + \sqrt{|J|} \quad (2)$$

where  $I$  and  $J$  are linear combinations of tripartite probability distributions (see Methods for their definitions).  $\mathcal{B} > 1$  indicates the rejection of bilocal models.

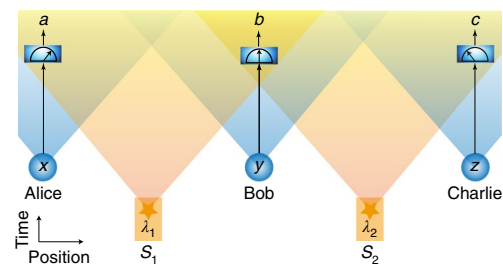


**Fig. 1 | Space-time diagram of the simplest quantum network.** The network has two sources distributing entanglement to three nodes, with the shaded areas indicating light cones.

<sup>1</sup>National Laboratory for Physical Sciences at Microscale and Department of Modern Physics, Shanghai Branch, University of Science and Technology of China, Shanghai, China. <sup>2</sup>CAS Center for Excellence and Synergetic Innovation Center in Quantum Information and Quantum Physics, Shanghai Branch, University of Science and Technology of China, Shanghai, China. <sup>3</sup>State Key Laboratory of Functional Materials for Informatics, Shanghai Institute of Microsystem and Information Technology, Chinese Academy of Sciences, Shanghai, China. <sup>4</sup>Department of Physics and Astronomy, Shanghai Jiao Tong University, Shanghai, China. <sup>5</sup>These authors contributed equally: Qi-Chao Sun, Yang-Fan Jiang, Bing Bai. \*e-mail: [qiangzh@ustc.edu.cn](mailto:qiangzh@ustc.edu.cn); [fanjy@sustech.edu.cn](mailto:fanjy@sustech.edu.cn); [pan@ustc.edu.cn](mailto:pan@ustc.edu.cn)

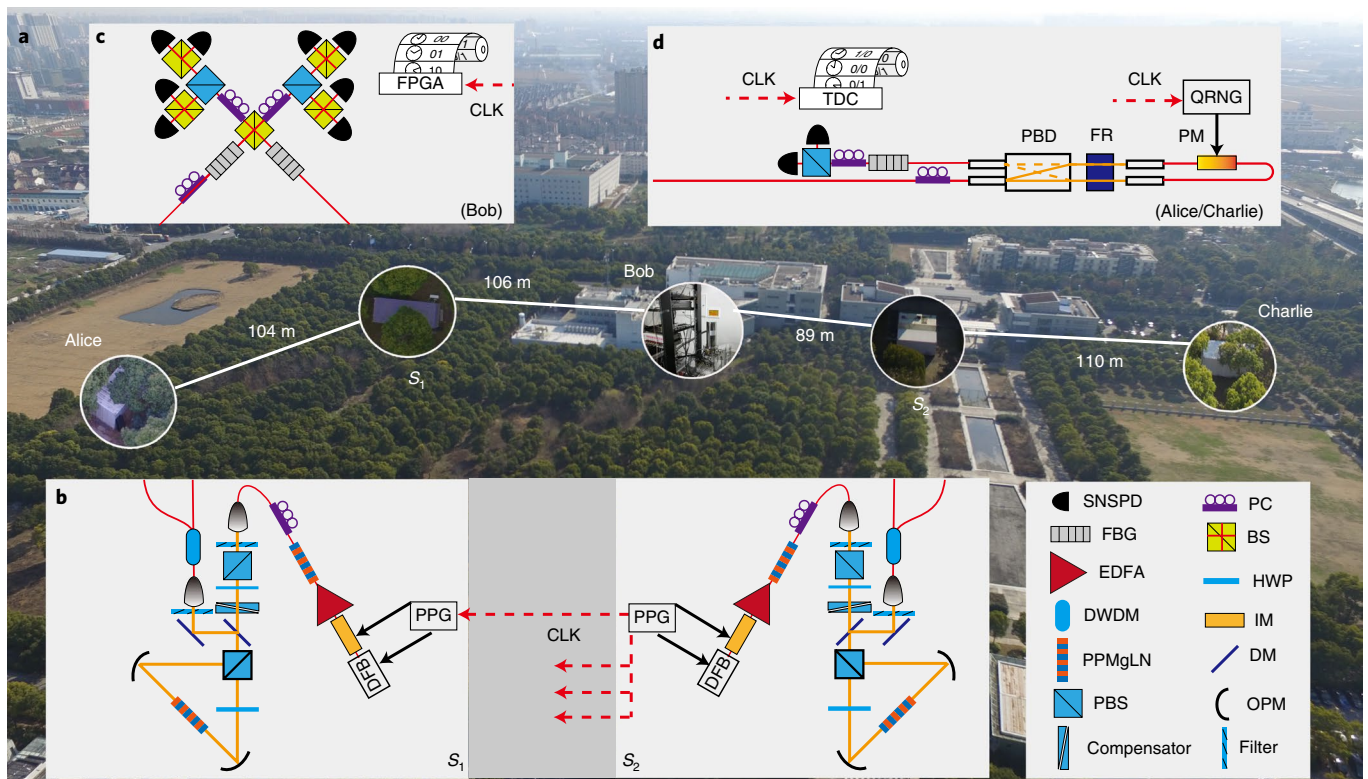


**Fig. 2 | Schematics for testing the bilocality in a network.** **a**, Bird's-eye view of the network with nodes for Alice, Bob and Charlie and two sources  $S_1$  and  $S_2$ . The length of the connecting fibre links (white lines) for Alice- $S_1$ ,  $S_1$ -Bob, Bob- $S_2$  and  $S_2$ -Charlie are 110.98 m, 124.52 m, 108.13 m and 124.55 m, respectively. **b**, In each source, the laser pulses from a 1,558 nm distributed feedback (DFB) laser are frequency-doubled in a periodically poled MgO doped lithium niobate (PPMgLN) crystal after passing through an erbium-doped fibre amplifier (EDFA). The produced 779 nm laser pulses create entangled photon pairs in the second PPMgLN crystal, which are collected into an optical fibre. In  $S_2$ , a 12.5 GHz microwave clock (pulse pattern generator, PPG) is used as the master clock, which sends synchronization signals (CLK) to all nodes in the network (red dashed lines). For details about the experimental realization see Supplementary Information. **c**, Bob performs the BSM with the combination of 50:50 BSs, PBSs and eight superconducting nanowire SPDs (SNSPDs). The photon detection results are analysed in real time and recorded by a field-programmable gate array (FPGA), which is synchronized by the CLK signals. **d**, Synchronized to the master clock, a quantum random number generator (QRNG) outputs a random bit to notify Alice (Charlie) to perform the single-photon polarization modulation (measurement setting choice) with a loop interferometer, which consists of a polarization beam displacer (PBD), a Faraday rotator (FR) and a phase modulator (PM) (see Methods). The SPD results are recorded by a time-to-digital converter (TDC), which is synchronized by the CLK signals. DWDM, dense wavelength-division multiplexer; OPM, off-axis parabolic mirrors; FBG, fibre Bragg grating.

Loophole-free violation of the Bell inequality for a two-party system is a formidable task in experimental physics, and was only accomplished after  $\sim 40$  years of persistent work from the first experiment<sup>18</sup>. An experimental test of quantum non-locality in a quantum network is further complicated by the causal structure of the network. In addition to simultaneously closing the locality, detection and measurement independence loopholes as for a loophole-free Bell test experiment, all quantum state creation events at separate quantum sources in the network must be independent with respect to each other. Although existing experimental studies of bilocality have demonstrated the general strategy to test quantum non-locality in a network<sup>19–21</sup>, the critical ingredients—that is, closing the loopholes, which is known to be experimentally challenging—remain to be completed. Here we report an experimental study of bilocality with locality, measurement independence and quantum source independence loopholes closed simultaneously in a single quantum network experiment.

We constructed the network in the Shanghai campus of the University of Science and Technology of China, where sources  $S_1$  and  $S_2$  distribute polarization-entangled photon pairs generated via a spontaneous parametric downconversion (SPDC) process to three nodes (see Fig. 2a and Methods for details). Bob sandwiches polarization beamsplitters (PBSs) between 50:50

beamsplitters (BSs) to realize the BSM (Fig. 2c), with which we can read the path, polarization and photon number information about the incoming two photons. The two photons in Bell state  $|\Psi^-\rangle = \frac{1}{\sqrt{2}}(|H\rangle|V\rangle - |V\rangle|H\rangle)$  exit from different ports of the first BS, the two photons in Bell state  $|\Psi^+\rangle = \frac{1}{\sqrt{2}}(|H\rangle|V\rangle + |V\rangle|H\rangle)$  exit from different ports of the PBS, and the two photons in Bell state  $|\Phi^+\rangle$  or  $|\Phi^-\rangle$  bunch together and are resolved with 50% of success by the photon-number-resolving detection process (implemented by the last BS and two single-photon detectors, SPDs). That is, only Bell states  $|\Psi^-\rangle$ ,  $|\Psi^+\rangle$  and a group of Bell states  $\{|\Phi^+\rangle, |\Phi^-\rangle\}$  can be discriminated in the BSM with linear optics<sup>22</sup>. For such a BSM with one fixed input and three outputs, we examined the bilocal relation  $\mathcal{B}_{13}$  (see Methods). To maximize the value of  $\mathcal{B}_{13}$ , we use bases  $\hat{A}_0 = \hat{C}_0 = (\sqrt{2}\sigma_z + \sigma_x)/\sqrt{3}$  and  $\hat{A}_1 = \hat{C}_1 = (\sqrt{2}\sigma_z - \sigma_x)/\sqrt{3}$ , respectively, in Alice and Charlie's single-photon polarization measurements, where  $\sigma_x$  and  $\sigma_z$  are two Pauli matrices. Assume that the photons emitted by each source are described by the Werner state,  $\rho_i^w = v_i|\Phi^+\rangle\langle\Phi^+| + \frac{1-v_i}{4}\mathbf{I}$ , where  $v_i = 1, 2$  is the visibility for the state created, respectively, by  $S_1$  and  $S_2$ , and  $\mathbf{I}$  is the identity operator, quantum theory predicts  $\mathcal{B}_{13} > 1$  for swapped entanglement visibility  $v > 2/3$  ( $v = v_1 v_2$ ). We note that  $v > 1/\sqrt{2}$  is required to violate the Clauser–Horne–Shimony–Holt (CHSH) inequality<sup>23</sup>.

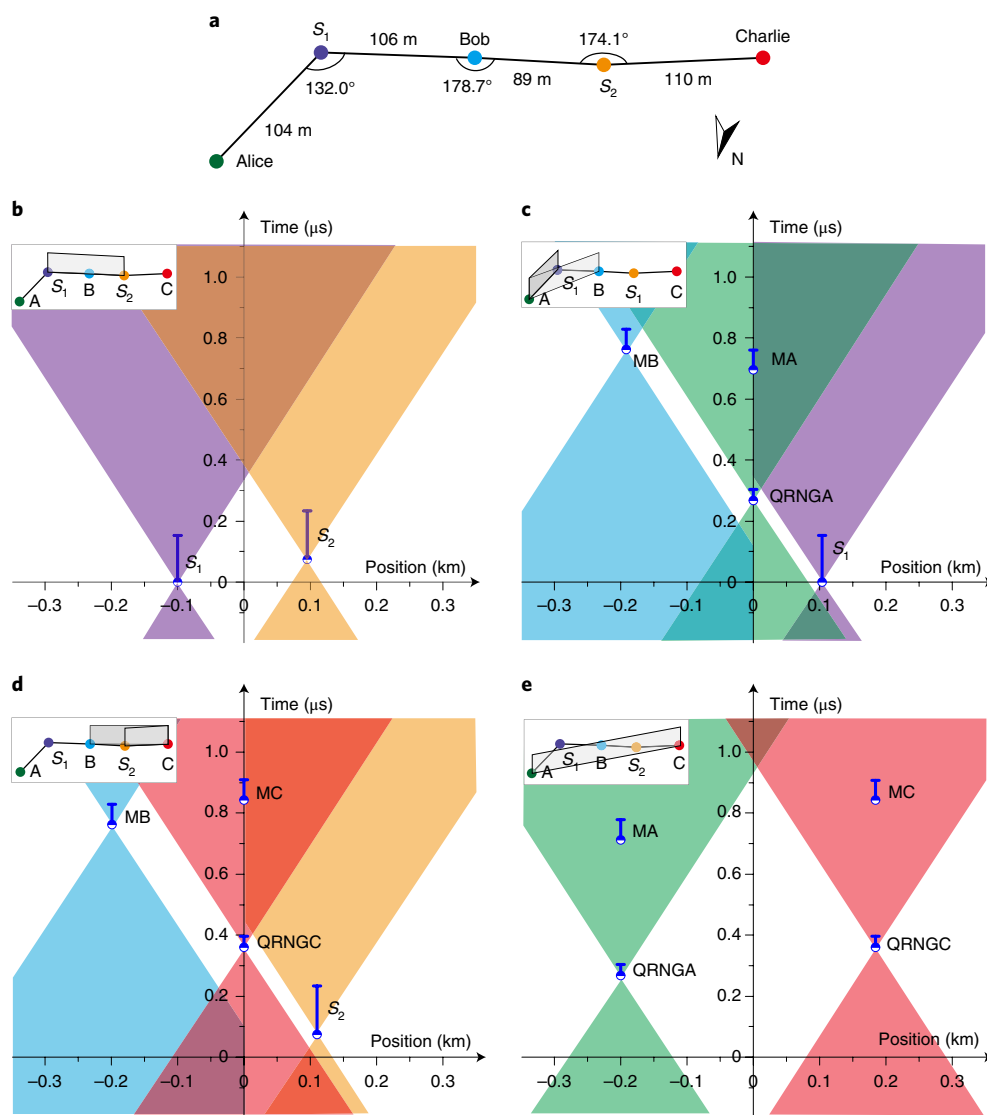


**Fig. 3 | Space-time configuration of relevant events in each experimental trial. a**, Relative spatial configuration of the two-source and three-node network. **b–e**, Space-time diagrams of the relationship between important events in the nodes, as indicated in the insets. Origins of the axes are displaced to reflect the relative space and time difference between them. **b**, Space-like separation between state emission events in the two sources,  $S_1$  and  $S_2$ . **c**, Space-like separation between the quantum random number generation event of Alice (QRNGA) and the measurement event by Bob (MB) is shown on the left-hand side of the vertical axis, with the state emission event in the nearest source on the right-hand side of the vertical axis. **d**, Similar to **c**, QRNGC denotes the quantum random number generation event of Charlie. **e**, Space-like separation between the two quantum random generation events and space-like separations between a quantum random number generation event and the measurement event between node Alice and node Charlie. Blue vertical bars indicate the time elapsing for events, with start and end marked by circles and horizontal dashes, respectively. All the time-space relations are drawn to scale. Therefore, further time-space relations can be inferred; for example, the space-like separation of QRNGA– $S_2$  and QRNGC– $S_1$  is implied by **c,d**. For details see Supplementary Information.

Creating a quantum state independently in each source is a prerequisite to construct a quantum network. Previous works have demonstrated possible ways to realize independent sources<sup>9,12,24</sup>. Our solution to this problem is largely inspired by the realization of a quantum random number generator (QRNG) based on vacuum noise<sup>25</sup>. The generated random bits are assumed to be created locally and independently and are private and uniform for the use of input settings in loophole-free Bell test experiments<sup>9–11</sup>. We use these QRNGs to assign input settings in the single photon state measurements in this experiment. We use the same mechanism to switch an electrically driven laser diode from much below the threshold to well above the threshold in each duty cycle such that the phase of each generated laser pulse is randomized in each source<sup>25</sup>. The two SPDC processes in the two sources are therefore disconnected.

In this way, we close the independent source loophole. Microwave clocks are used as a time reference to synchronize all events in the experiment (see Supplementary Information). With the time reference, each source generates laser pulses for the creation of entangled photon pairs via SPDC process; this is also the earliest time for the birth of a local hidden variable in that duty cycle.

We assign a duty cycle as an experimental trial. To satisfy the requirements of measurement independence and the locality constraint, we require space-like separation between relevant events in each experimental trial, as shown in Fig. 3: (1) space-like separation between the two state-emission events in sources  $S_1$  and  $S_2$ ; (2) space-like separation between the events of Alice (Charlie) completing the quantum random number generation for measurement setting choice and the state emission events in sources  $S_1$  and  $S_2$ ; (3) space-like

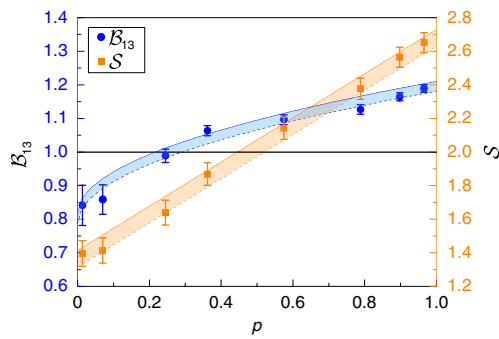


**Fig. 4** |  $B_{13}$  and  $S$  versus noise parameter  $p$ . The filled blue circles and filled orange squares show  $B_{13}$  and  $S$  measured in the experiment, respectively. Each data point represents an accumulation time of 8,000 s in the experiment. The error bars indicate 1 s.d., assuming Poisson statistics. The blue- and orange-shaded areas represent the theoretical expected range of the experimental value by considering the noise in quantum sources. We have considered white noise and colour noise in the quantum sources; the upper bound denotes that noise only comes from colour noise (solid lines) and the lower bound denotes that noise only comes from white noise (dashed lines) (see Supplementary Information).

separation between the events of Alice (Charlie) completing the quantum random number generation for measurement setting choice and the events of completing single photon detection by Bob and Charlie (Alice); (4) space-like separation between the two events of random bit generation for measurement setting choices for Alice and Charlie (see Supplementary Information for details). To realize the fast measurement setting choice, we implement a high-speed high-fidelity single-photon polarization modulation with a loop interferometer as shown in Fig. 2d (see Methods for details). We achieve single photon polarization state modulation at a rate of 250 MHz and with a fidelity of  $99.0 \pm 0.2\%$  with random inputs.

As a reliability check before performing the experimental test of bilocal hidden variable models, we measured the two-photon interference visibility to be greater than 97% for states prepared by both sources, and we obtained a fitted visibility of  $96.5 \pm 1.6\%$  in the Hong–Ou–Mandel measurement with photons from the two independent sources<sup>26</sup>. We attribute the imperfect visibility mainly to the multi-photon pair events in the SPDC process. The fourfold coincidence count rate is about 1 per second in the experiment.

We measure  $B_{13} = 1.181 \pm 0.004$  in the experiment, which exceeds the bound ( $B_{13} \leq 1$ ) of bilocal hidden variable models by 45 standard deviations. We also measure a CHSH game value of  $S = 2.652 \pm 0.059$  in the Bell inequality test after entanglement swapping (see Methods), which exceeds the bound ( $S \leq 2$ ) of local hidden variable models by 11 standard deviations. We study the response of both parameters to the influence of noise by delaying a single photon pulse with respect to the other in the BSM from 0 (corresponding to noise parameter  $p = 1$ ) to a significant level ( $p < \frac{1}{2}$ ) (see Supplementary Information for details). The noise factor  $p$  actually characterizes the interference visibility. As shown in Fig. 4, the values of both  $B_{13}$  and  $S$  decrease with  $p$ . We also take the noise in the creation of the two-photon state into consideration and estimate the upper and lower bounds (shaded areas, Fig. 4). We notice that  $B_{13}$  remains above 1, even at a significant noise level, where  $S < 2$ . The experimental results are consistent with the theoretical results; for example, for the maximum violations in our experiment, the measured values  $B_{13} = 1.181 \pm 0.004$  and  $S = 2.652 \pm 0.059$  are within the expected ranges indicated by the shaded areas—(1.174, 1.203) and (2.585, 2.684), respectively. Compared to their ideal maximum violation values  $\sqrt{3/2}$  and  $2\sqrt{2}$ , the relative deviation of the expected range of  $B_{13}$  is smaller than

that of  $S$ . This also confirms the theoretical prediction that the rejection of bilocal hidden variable models is more noise tolerant (see Supplementary Information for details).

We highlight several important achievements in this experiment. By periodically bringing the laser from spontaneous emission to stimulated emission to output laser pulses with randomized phases for the SPDC process in each source, we close the independent source loophole. We use the same mechanism to generate random bits for measurement setting choices. By separating the random bit generation events space-like from the events of creating entanglement in the sources, we close the measurement independence loophole<sup>10,11</sup>. We close the locality loophole similarly. The detection loophole may be closed in the future with improved SPD efficiency. One could also follow the strategy adopted in a recent loophole-free Bell test experiment, which is to adopt cosmic randomness to exclude the concern of a common past to a certain extent<sup>27,28</sup>. One should keep in mind that it is impossible to rule out all conceivable local-realist theories<sup>2</sup>, as the local hidden variables could have been correlated at the birth of the universe. However, it is a reasonably good assumption that local hidden variables are created together with the creation of quantum entanglement as in the loophole-free Bell test experiments<sup>9–12</sup>. We remark that the demonstrated experimental techniques may be used to explore quantum networks with more advanced topological structures, for which one may expect a rich class of physics<sup>14,16,29–31</sup> as well as novel applications, for example, device-independent quantum information processing in quantum networks<sup>5</sup>.

### Online content

Any methods, additional references, Nature Research reporting summaries, source data, statements of code and data availability and associated accession codes are available at <https://doi.org/10.1038/s41566-019-0502-7>.

Received: 22 June 2018; Accepted: 3 July 2019;

Published online: 26 August 2019

### References

- Liao, S.-K. et al. Satellite-relayed intercontinental quantum network. *Phys. Rev. Lett.* **120**, 030501 (2018).
- Brunner, N., Cavalcanti, D., Pironio, S., Scarani, V. & Wehner, S. Bell nonlocality. *Rev. Mod. Phys.* **86**, 419–478 (2014).
- Vazirani, U. & Vidick, T. Fully device-independent quantum key distribution. *Phys. Rev. Lett.* **113**, 140501 (2014).
- Colbeck, R. A. *Quantum and Relativistic Protocols for Secure Multi-party Computation*. PhD thesis, Univ. Cambridge (2007).
- Lee, C. M. & Hoban, M. J. Towards device-independent information processing on general quantum networks. *Phys. Rev. Lett.* **120**, 020504 (2018).
- Branciard, C., Gisin, N. & Pironio, S. Characterizing the nonlocal correlations created via entanglement swapping. *Phys. Rev. Lett.* **104**, 170401 (2010).
- Einstein, A., Podolsky, B. & Rosen, N. Can quantum-mechanical description of physical reality be considered complete? *Phys. Rev.* **47**, 777–780 (1935).
- Bell, J. S. On the Einstein–Podolsky–Rosen paradox. *Physics* **1**, 195–200 (1964).
- Hensen, B. et al. Loophole-free Bell inequality violation using electron spins separated by 1.3 kilometres. *Nature* **526**, 682–686 (2015).
- Giustina, M. et al. Significant-loophole-free test of Bell’s theorem with entangled photons. *Phys. Rev. Lett.* **115**, 250401 (2015).
- Shalm, L. K. et al. Strong loophole-free test of local realism. *Phys. Rev. Lett.* **115**, 250402 (2015).
- Rosenfeld, W. et al. Event-ready Bell test using entangled atoms simultaneously closing detection and locality loopholes. *Phys. Rev. Lett.* **119**, 010402 (2017).
- Chaves, R., Kueng, R., Brask, J. B. & Gross, D. Unifying framework for relaxations of the causal assumptions in Bell’s theorem. *Phys. Rev. Lett.* **114**, 140403 (2015).
- Chaves, R. Polynomial Bell inequalities. *Phys. Rev. Lett.* **116**, 010402 (2016).
- Rosset, D. et al. Nonlinear Bell inequalities tailored for quantum networks. *Phys. Rev. Lett.* **116**, 010403 (2016).
- Fritz, T. Beyond Bell’s theorem II: scenarios with arbitrary causal structure. *Commun. Math. Phys.* **341**, 391–434 (2016).
- Żukowski, M., Zeilinger, A., Horne, M. & Ekert, A. ‘Event-ready-detectors’ Bell experiment via entanglement swapping. *Phys. Rev. Lett.* **71**, 4287–4290 (1993).
- Aspect, A., Grangier, P. & Roger, G. Experimental tests of realistic local theories via Bell’s theorem. *Phys. Rev. Lett.* **47**, 460–463 (1981).

19. Carvacho, G. et al. Experimental violation of local causality in a quantum network. *Nat. Commun.* **8**, 14775 (2017).
20. Saunders, D. J., Bennet, A. J., Branciard, C. & Pryde, G. J. Experimental demonstration of nonbilocl quantum correlations. *Sci. Adv.* **3**, e1602743 (2017).
21. Andreoli, F. et al. Experimental bilocality violation without shared reference frames. *Phys. Rev. A* **95**, 062315 (2017).
22. Weinfurter, H. Experimental Bell-state analysis. *Europhys. Lett.* **25**, 559–564 (1994).
23. Clauser, J. F., Horne, M. A., Shimony, A. & Holt, R. A. Proposed experiment to test local hidden-variable theories. *Phys. Rev. Lett.* **23**, 880–884 (1969).
24. Sun, Q.-C. et al. Quantum teleportation with independent sources and prior entanglement distribution over a network. *Nat. Photon.* **10**, 671–675 (2016).
25. Abellán, C., Amaya, W., Mitrani, D., Pruneri, V. & Mitchell, M. W. Generation of fresh and pure random numbers for loophole-free Bell tests. *Phys. Rev. Lett.* **115**, 250403 (2015).
26. Hong, C., Ou, Z. & Mandel, L. Measurement of subpicosecond time intervals between two photons by interference. *Phys. Rev. Lett.* **59**, 2044–2046 (1987).
27. Handsteiner, J. et al. Cosmic Bell test: measurement settings from Milky Way stars. *Phys. Rev. Lett.* **118**, 060401 (2017).
28. Li, M.-H. et al. Test of local realism into the past without detection and locality loopholes. *Phys. Rev. Lett.* **121**, 080404 (2018).
29. Tavakoli, A., Skrzypczyk, P., Cavalcanti, D. & Acín, A. Nonlocal correlations in the star-network configuration. *Phys. Rev. A* **90**, 062109 (2014).
30. Andreoli, F., Carvacho, G., Santodonato, L., Chaves, R. & Sciarrino, F. Maximal qubit violation of n-locality inequalities in a star-shaped quantum network. *New J. Phys.* **19**, 113020 (2017).
31. Gisin, N. The elegant joint quantum measurement and some conjectures about n-locality in the triangle and other configurations. Preprint at <http://arxiv.org/abs/1708.05556> (2017).

## Acknowledgements

We thank Y. Liu, Y. Li and Y.-Q. Nie for enlightening discussions, Y.-L. Mao for assistance, K.-X. Yang for help with the aerial photographs and Quantum Ctek for providing the components used in the QRNGs. This work was supported by the National Key R&D Program of China (2017YFA0303900, 2017YFA0304000), the National Natural Science Foundation of China and the Chinese Academy of Sciences.

## Author contributions

Q.-C.S., Q.Z., J.F. and J.-W.P. conceived and designed the experiments. B.B. and J.Z. built the QRNGs. W.Z., H.L., L.Y. and Z.W. fabricated the SNSPDs. Q.-C.S. and Y.-F.J. built the experimental network and carried out the experiment. X.J. and X.C. provided experimental assistance. Q.-C.S. and Y.-F.J. analysed the data. Q.-C.S., Q.Z., J.F. and J.-W.P. wrote the manuscript, with input from all authors.

## Competing interests

The authors declare no competing interests.

## Additional information

**Supplementary information** is available for this paper at <https://doi.org/10.1038/s41566-019-0502-7>.

**Reprints and permissions information** is available at [www.nature.com/reprints](http://www.nature.com/reprints).

**Correspondence and requests for materials** should be addressed to Q.Z., J.F. or J.-W.P.

**Publisher's note:** Springer Nature remains neutral with regard to jurisdictional claims in published maps and institutional affiliations.

© The Author(s), under exclusive licence to Springer Nature Limited 2019

## Methods

**Polarization-entangled photon-pair source.** In each of the two sources  $S_1$  and  $S_2$ , as shown in Fig. 2a, the DFB laser emits a 2 ns laser pulse (central wavelength 1,558 nm) at a repetition rate of 250 MHz. A 40 GHz intensity modulator (IM) is used to carve the 2 ns laser pulses into 90 ps laser pulses. Both the DFB laser and the IM are driven by a PPG. The laser pulses are amplified by an EDFA and fed into a PPMgLN crystal for second harmonic generation (SHG). The SHG pulses are coupled into a 780 nm single-mode fibre. The residual pump laser pulses are highly attenuated and then output to free space through a fibre coupler. After being filtered by an 855 nm bandpass filter, the 779 nm laser pulses are used to pump a 2.5-cm-long PPMgLN crystal placed inside a polarization Sagnac loop. The focal length of the OPM is 101.6 mm and the beam diameter at the beam waist is 108  $\mu\text{m}$ . Photon pairs are generated via the type-0 SPDC in the PPMgLN crystal. Two dichroic mirrors are used to separate the photon pairs from the pump pulses. After passing through a silicon plate, the photons are collected into the fibre. The photon pairs with wavelengths at 1,560 nm and 1,556 nm are selected using a set of DWDM filters. To suppress the distinguishability between photons from separate sources in the network, we pass photons through inline 3.3 GHz FBGs to suppress the spectral distinguishability. The 133 ps coherence time of single photons is much longer than the pump pulse duration, which, together with the high bandwidth synchronization (with an uncertainty of 4 ps), suppress the temporal distinguishability; the good fibre optical mode eliminates the spatial distinguishability.

**Polarization modulation.** A high-speed high-fidelity single-photon polarization modulation device is a critical element in the realization of the quantum network. We present such an implementation based on the design of a loop interferometer. As shown in Fig. 2d, a single photon incident onto the loop has its two orthogonal polarization components exit at different ports of the PBD. With polarization rotated by 45° by the FR and aligned with the slow axis of a polarization-maintaining fibre, both polarization components are coupled into this fibre to propagate in opposite directions in the loop. A phase modulator (PM) is displaced from the middle position by 26 cm to create a relative delay of  $\sim 1.3$  ns between the arrival times of the two counter-propagating components at the PM such that the PM can manipulate the phase to only one of them. The two components interfere at the PBD and exit as a single photon pulse with a modulated polarization state.

**Bilocal correlation function  $\mathcal{B}_{13}$  and Bell correlation function  $\mathcal{S}$ .** In our experiment, we examine  $\mathcal{B}_{13}$  in the case where Bob performs the one-fixed-input and three-output BSM<sup>32</sup>. Quantities  $I$  and  $J$  in equation (2) are defined as

$$\begin{aligned} I &= \frac{1}{4} \sum_{x,z} \langle A_x B^0 C_z \rangle_{P_{13}} \\ J &= \frac{1}{4} \sum_{x,z} (-1)^{x+z} \langle A_x B^1 C_z \rangle_{P_{13}, b^0=0} \end{aligned} \quad (3)$$

where the BSM outputs are denoted as  $\mathbf{b} = b^0 b^1 = 00, 01$  and  $\{10 \text{ or } 11\}$  for  $|\Psi^-\rangle$ ,  $|\Psi^+\rangle$  and  $\{|\Phi^-\rangle \text{ or } |\Phi^+\rangle\}$ , respectively, and the tripartite correlation terms are defined as

$$\begin{aligned} \langle A_x B^0 C_z \rangle_{P_{13}} &= \sum_{a,c} (-1)^{a+c} [P_{13}(a, 00, c|x, z) + P_{13}(a, 01, c|x, z) \\ &\quad - P_{13}(a, \{10 \text{ or } 11\}, c|x, z)] \\ \langle A_x B^1 C_z \rangle_{P_{13}, b^0=0} &= \sum_{a,c} (-1)^{a+c} [P_{13}(a, 00, c|x, z) - P_{13}(a, 01, c|x, z)] \end{aligned} \quad (4)$$

where the probability distribution  $P_{13}$  is the correlation shared by Alice, Bob and Charlie.

In the Bell test, we only use the results with BSM outcome  $|\Psi^-\rangle$ . The measurement bases of Alice and Charlie are  $\hat{A}_0 = \sigma_z$  or  $\hat{A}_1 = \sigma_x$  and  $\hat{C}_0 = (\sigma_z + \sigma_x)/\sqrt{2}$  or  $\hat{C}_1 = (\sigma_z - \sigma_x)/\sqrt{2}$ , respectively. The CHSH value<sup>23</sup> is calculated as

$$\mathcal{S} = |\langle A_0 C_0 \rangle_{\mathbf{b}=00} + \langle A_0 C_1 \rangle_{\mathbf{b}=00} + \langle A_1 C_0 \rangle_{\mathbf{b}=00} - \langle A_1 C_1 \rangle_{\mathbf{b}=00}| \quad (5)$$

where the correlation terms are defined as

$$\langle A_x C_z \rangle_{\mathbf{b}=00} = \sum_{a,c} (-1)^{a+c} P_{13}(a, c|x, z, \mathbf{b}=00).$$

## Data availability

The data that support the plots within this paper and other findings of this study are available from the corresponding author upon reasonable request.

## References

- Branciard, C., Rosset, D., Gisin, N. & Pironio, S. Bilocal versus nonbilocal correlations in entanglement-swapping experiments. *Phys. Rev. A* **85**, 032119 (2012).